International Journal of Engineering Trends and Technology
ISSN: 2231–5381 / https://doi.org/10.14445/22315381/IJETT-V72I4P106

Volume 72 Issue 4, 51-66, April 2024

Original Article

Stability Analysis of Grid-Integrated PV Systems

Gaurav B. Patil[1], Santosh S. Raghuwanshi[2], L. D. Arya[3]

[1,2,3]*Electrical Engineering, Medi-caps University, Indore, Madhya Pradesh, India.*

[1]*Corresponding Author : gauravpatilee@gmail.com*

Received: 22 November 2023 Revised: 20 February 2024 Accepted: 01 April 2024 Published: 24 April 2024

Abstract *- In recent years, the integration of renewable energy sources into the grid has increased exponentially. However, one significant challenge in integrating these renewable sources into the grid is intermittency and instability. The system's instability regarding voltage, frequency, and rotor angle is of utmost importance while doing this integration. To address this challenge, one must consider a test system and analyze it to suggest remedies to overcome the effect caused by integration. In the present work, Grid Integrated PV systems have been comparatively analyzed before and after the application of PV and then using various controller models of Type 1, 2, and 3 in ETAP Software, and the results state promising recommendations for the appropriate FACTS device to use with the test at hand for the best operational quick results. The simulation results clearly show that the system without FACTS exceeds the frequency limit and that using FACTS with the suggested converter brings them close to the appropriate value. Overall, the test system's transient stability is analyzed to improve the performance of integrated systems.*

Keywords *- Voltage stability, Renewable energy Photovoltaic systems, Flexible AC transmission device, Static VAR compensator*.

1. Introduction

The increasing global demand for electricity is placing increasing environmental pressure on conventional energy sources such as coal, crude oil and nuclear energy. Global warming, which is exacerbated by energy emissions from the combustion of fossil fuels, is directly responsible for this. More than ninety percent of the world's primary energy consumption in 2023 came from the use of fossil fuels. It is projected that as fossil fuel sources become less prevalent, the use of renewable energy will increase. Generator torque is produced by the wind turbine using the acquired wind energy. The alternator converts the torque into AC electrical energy, which is then transferred to the grid. A 1 MW wind farm can liberate 1.5 Lakh of CO_2, 6500 Kg of SO_2, and 32000 Kg of nitrogen oxides each year [1, 2]. PV generation is a method that uses solar cells in photovoltaic (PV) cells to convert solar into electrical energy. Solar power generation is gaining popularity as a renewable energy source these days. Solar photovoltaics produce power mainly in two ways.

The usage of an independent system is one approach. Batteries or other types of storage may be used to store energy for usage by local loads. Feeding the grid with electricity produced by solar panels is another way to use solar energy [3]. Subsequently, it is utilized by further loads linked to that feeder, a feeder in the vicinity, or a feeder situated farther from the grid. As option two utilizes the grid's current infrastructure, it is the most popular. As a result, unlike mode 1, there are no extra expenses or storage needs. The key problem with this type of grid integration for PV systems is grid stability; even if it can use the existing infrastructure, there can still be issues with grid protection and operation [4]. The two primary subcategories of stability research are Transient Stability (TS) and steady-state stability.

Steady-State Stability (SSS) is the capacity of the electrical system to return to synchronism after mild and moderate failure, like a progressive power increase. TS analysis examines a power system's capacity to remain synchronized when confronted with a substantial disturbance, such as a three-phase fault, the abrupt cutting off of a transmission line, or the abrupt increase or decrease of loads [5-9].

Results from investigations into this type of stability can help establish two important metrics: the voltage level of the electrical system and the critical clearing time (tCCT) of the circuit breakers. One key component of TS research for maintaining power system transient stability is the tCCT [10]. The idea of tCCT is related to TS. The time required for the power system to maintain transient stability, abbreviated as tCCT, is highest between the start of the fault and its clearing. When all three circuit breaker poles are fully open, the clearing time is the period that elapses between the disturbance and that moment. By keeping the fault time interval extended until the system becomes unstable, we can determine the crucial clearing time. Reducing the protection system rating, lowering the cost, and increasing the reliability

of the protection system can be achieved by increasing the tCCT [11]. This study aims to improve the efficiency of solar PV systems that are connected to the grid by using different FACTS devices. Several mistakes were carried out on ETAP systems with and without solar PV. In ETAP, both with and without solar PV, various errors were executed. The system's performance was then evaluated both before and after solar PV installation. The ability of the FACTS devices to repair the system was put to the test through numerous tests. The advantage of being able to control "fast" system oscillations is a feature of FACTS controllers. By adequately simulating these controllers in transient stability with the Test system, it would be interesting to determine any other potential advantages of these controllers in voltage stability research.

To evaluate the advantages and disadvantages of these controllers in research on voltage stability and suggest the best solutions for enhancing voltage stability for the evaluation of transient and steady-state stability for different FACTS controllers, it was important to build adequate models.

Additionally, this study contrasts and recommends the best FACTS device for a use case related to the test system. Specifically focusing on frequency and overall stability, this work and its result seek to outline the substantial influence of integration. But the suggested fact is that controllers get over that frequency loss and, in the end, stabilize to a large degree. The fundamental basis of various power system stability will be presented in Sections 2 and 3, along with a brief discussion of the transient stability equations linked to fault clearance. The following Section 4 provides extensive modeling of solar PV systems. Section 5 will give a precise picture of the proposed system, and Section 6 will present all of the experimental results analysis taking diverse instances into account. Section 7 concludes the paper with a discussion.

2. Classification of Power System Stability

Maintaining synchronous operation in the Power System Network (PSN), or rotor angle stability, has historically been the problem with power system stability. PSN instability can also happen without a loss of synchronization. The issue of rotor angle stability involves the [12] investigation of electro-mechanical oscillations. A power system is considered voltage stable if the bus voltages following a disturbance are comparable to the voltages under normal operating conditions. A power system is considered unstable when the voltages drop suddenly due to equipment failure or an increase in load. Rotor angle stability and voltage stability are connected. Reactive power control, meanwhile, impacts both voltage and rotor angle stability. Rotor angle stability is primarily generation-dependent, whereas voltage stability is primarily load-dependent. One may say that problems with angle stability arise when the balance between actual power generation and load is not zero [13-16]. However, when the imaginary power Q of generation and load is a non-zero value, then the system has voltage instability issues [17].

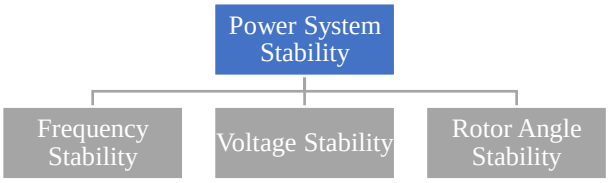

Fig. 1 Classification of power system stability

2.1. Rotor Angle Stability

The ability of the PSN-connected synchronous machines to keep pace with one another, or in synchronism, is known as the rotor angle stability of EPS [1,2]. The investigation of electro-mechanical oscillations is necessary for the rotor angle stability problem. The way a synchronous machine's power output varies with rotor oscillation is the key component of rotor angle stability. Either SSS or TS could apply here [18].

2.2. Frequency Stability

The ability of PSN to retain constant frequency following a serious system upset that causes a sizable imbalance between generation and load is referred to as frequency stability. It depends on the PSN's capacity to keep or restore the balance between the load side and the generating unit of the electrical power system with minimal loss. According to Kundur [1,2], inadequate generating reserve, poorly coordinated control and protection systems, or inadequate equipment reactions are the main causes of frequency stability issues.

2.3. Voltage Stability

Voltage stability is concerned with the ability of the PSN to maintain acceptable voltage levels at all buses in the system under normal operating conditions and after being subjected to disturbances. To determine the stability limits and margin, it is necessary to determine the voltage level at each bus under various loading scenarios. Numerous studies are being conducted worldwide due to voltage instability's significant economic and social impact on utility companies and their consumers [19-21].

2.3.1. Large-Disturbance Voltage Stability

It deals with the system's capacity to keep voltages constant in the wake of significant disturbances such *as* system errors, power outages, or circuit contingencies.

2.3.2. Small-disturbance Voltage Stability

It describes the system's capacity to keep stable voltages under the influence of minor disturbances such as gradual variations in system load.

3. Transient Stability and Critical Clearing Time

The capability of the system to return to synchronization following substantial disturbances, such as the loss of a generating unit, switching of lines, massive shifts in load, or breakdowns, is known as Transient Stability (TS). Initial swing stability is the name given to it and is also defined in

[22] as stability that maintains the synchronizing torque. On the other hand, [23] describes a system's ability to keep an operational point that remains constant, notwithstanding disruptions that alter the topology of the system. To properly examine TS, the Equal Area Criterion (EAC) and numerical integration techniques—both referred to as time domain approaches—are routinely used. [24-26] To assess the system's resilience, time domain analysis is used to observe the CCT of the system.

There is an essential viewpoint, or critical angle, for resolving the issue to maintain the equal area condition. Known as critical clearance, this angle CCA and time CCT refers to the angle and corresponding time for eliminating the fault. In general, it is the time required to fix the issue before the system loses synchronization after the issue has been fixed. Through the use of EAC, CCT expression is mathematically derived in [26] the CCA (1) and (2) include the equations.

$$\delta cr = \frac{\omega s\, Pm}{4H} + tcr^2\, \delta_0 \quad (1)$$

$$tcr = \sqrt{\frac{4H(\delta cr - \delta 0)}{\omega s\, Pm}} \quad (2)$$

Where,

H, ωs, and Pm stand for the machine's mechanical power, synchronous speed, and constant of inertia. On the other hand, δcr and tcr represent the critical angle of clearing and the amount of time needed for it. Since the machine is operating at synchronous speed at that moment, δ0 represents the rotor angle. Equation (2) makes it evident that H, ωs, Pm δ0, and δcr are the major factors that affect CCT. However, factors like as machine type, fault location, load level, fault current strength, etc., can affect these properties.

After looking at some research papers [28–30] in this area, the summary states that an inverter-based control algorithm for setting up a PV controller that supports fast reactive power and has three active power control modes. It can operate effectively in various weather conditions and transient operational disturbances. Results show that transient stability does not improve with reconnecting large solar PV plants after faults, and voltage stability improves with fast reconnection of induction motors.

4. Modelling of a solar PV system

Solar photovoltaic (PV) arrays consist of multiple solar cells connected in series and Shunt Combination. The analogous circuit of the solar cell is shown by a single diode in Figure 2a. Figure 2b shows the equivalent circuit for a photovoltaic array consisting of series (Ns) and Shunt (Np) cells. The initial photocurrent (Iph) produced by the solar cell is the unit of measurement. ID denotes the current flowing ahead via the diode, D is the cell photocurrent, and Ish is the current through the shunt resistor. The resistive drop in the structure of the cell is caused by its inherent series resistance (Rse) and its parallel resistance (Rsh), respectively, which are responsible for the drop in the cell.

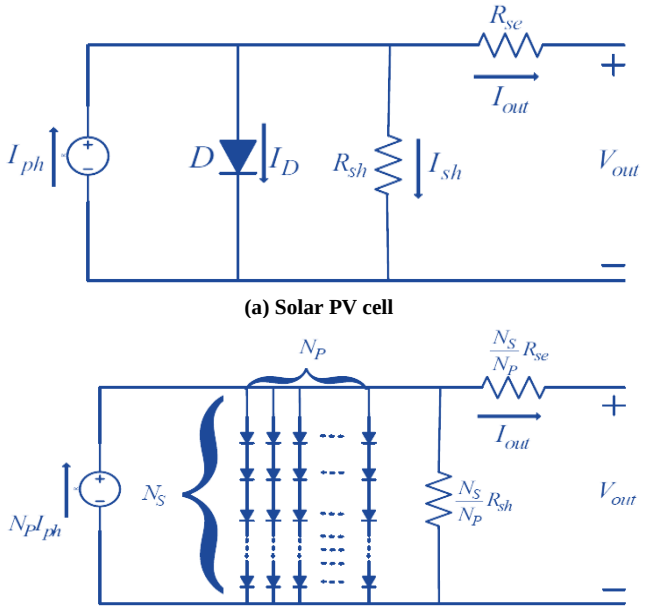

(a) Solar PV cell

(b) Solar PV module

Fig. 2 Equivalent Circuit of a PV Module and Solar PV Cell

When KCL is imposed on the above circuit in Figure 2a, which can also be used to determine the output current [27], I_{out}, will be

$$I_{out} = I_{ph} - I_0[\exp(q(V_{out}+I_{out}R_{se})/nkT)-1] - (V_{out}+I_{out}R_{se})/R_{sh} \quad (3)$$

The output current, Iout, are written [27] as:

$$I_{out} = N_p I_{ph} - N_p I_0[\exp(q(N_p V_{out}+N_s I_{out}R_{se})/nkT\, N_p N_s)-1] - (N_p V_{out}+ N_p I_{out}R_{se})/N_s R_{sh} \quad (4)$$

Where V_{out}, q, n, T, and k indicate output voltage, q charge on an e^-, ideality factor, and operational temperature. Boltzmann's constant, respectively.

The expression [27] for the temperature-dependent dark saturation current, I_o, is

$$I_0 = I_R \left(\frac{T}{T_R}\right)^3 exp\left[\frac{qE_G}{nk}\left(\frac{1}{T}-\frac{1}{T_R}\right)\right] \quad (5)$$

Where T_R and I_R are corresponding reference temperatures, reverse saturation current at standard operation condition, i.e. 25 degrees or 298 Kelvin, E_G represents bandgap energy. Another parameter, Iph, n, Rse, and Rsh, in the above Equations also depends on the operating temperature and radiation.

5. Proposed System

The ETAP tool was utilized to incorporate the Test System line diagram, which consists of two generators capacity of 10 MW. Both these generators are placed on either of the transmission networks. Four buses of voltages 11kv and 110kv (two of each, respectively), along with two transformers, can be seen in Figure 3.

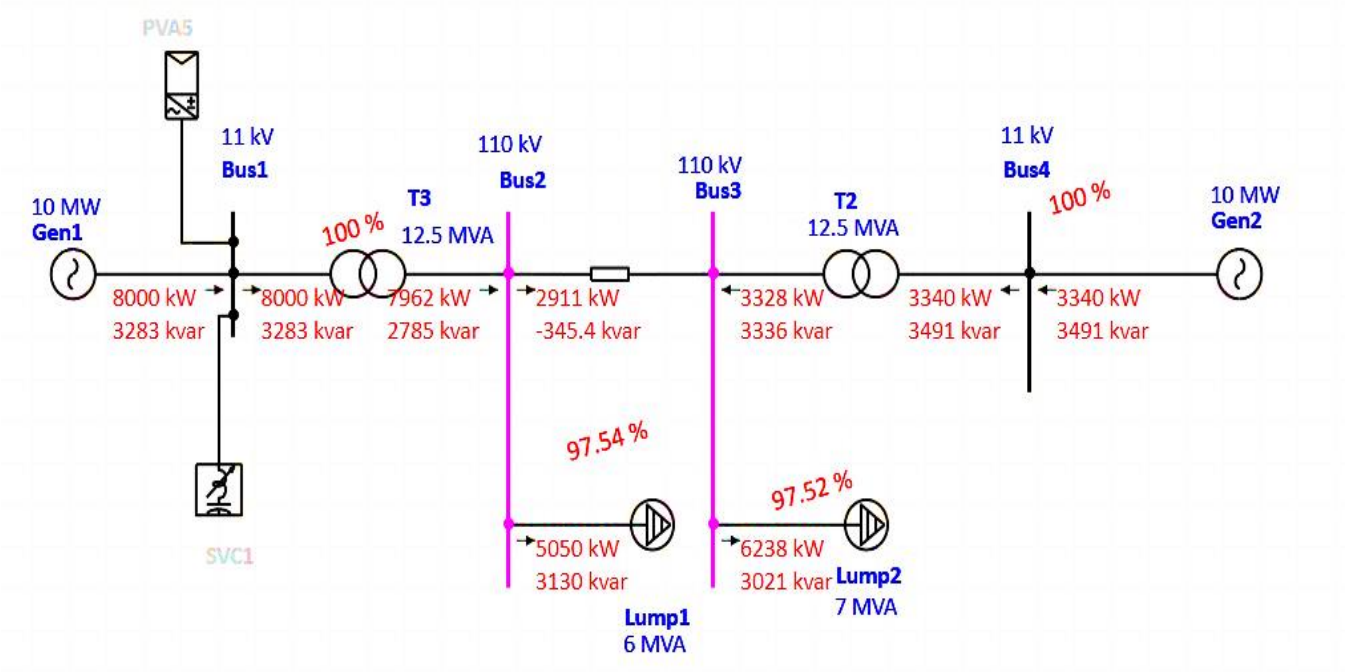

Fig. 3 Line Diagram of Test System in ETAP

In addition to this, Photovoltaic PV is connected at Bus Number 1 earlier, which has a capacity of 500 kW, which consists of 300 panels in series and 6 such arrays in parallel. Each panel can generate 282.5 watts of power with an open circuit voltage of 43.92Volt and a short circuit current of 8.4A.

Inverter used in this proposed system has a DC power rating of 555 kW. With an efficiency of 90% and a power factor close to unity, since PV system does not provide any reactive power support to the entire system. In addition to this, to mitigate adverse effects FACTS device, i.e. SVC, has been introduced into the test system can be seen at the bottom side of Figure 3.

Table 1 depicts various elements incorporated while designing the Test system, along with their detailed specification.

6. Results and Discussion

At first, ETAP was used to simulate the test system without including PV and FACTS. Where a system characteristic, such as the generator's speed and current, was measured and displayed against time, as depicted in Figure 4. The LLLG fault, in this instance, starts at 1 second and is cleared at 1.1 seconds. Up to 1555 rpm, the speed dramatically rose in magnitude. After that, the speed gradually drops until it returns to normal in 20 seconds.

The magnitude of the current simultaneously increased to roughly seven times its rated value, and it recovered in 3 seconds. Next, the system ran with added PV to the test system, which is seen in the line diagram close to the first generator. After that, the simulation was executed repeatedly to view the speed and current plots against the corresponding times, as shown in Figure 5.

The usual operating speed is noted to be disrupted by the addition of PV to the system more severely than it was previously; it almost reaches 1565 rpm before resuming within 8 seconds, and the current value reaches 1570 amps. It implies that the addition of the PV system has affected the system parameters i.e. current and generator speed.

Table 1. Elements of the Test System

S.N.	Elements	Specification	Quantity
1	Generators	10MW	02
2	Bus	11Kv and 110kV	04
3	Transformer	T1 and T2	02
4	PV	500Kw	01
5	FACTS (SVC)	Static VAR compensator	01

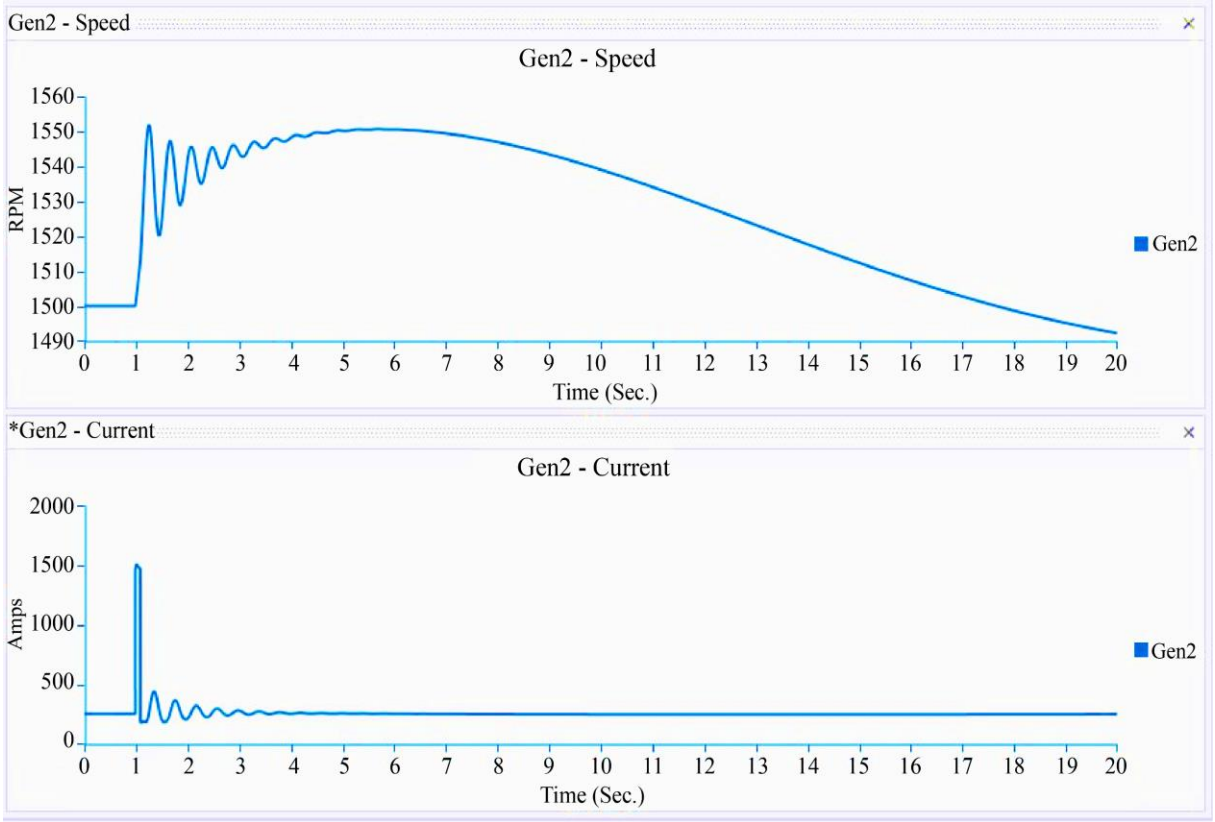

Fig. 4 Generator Parameters without PV FACTS

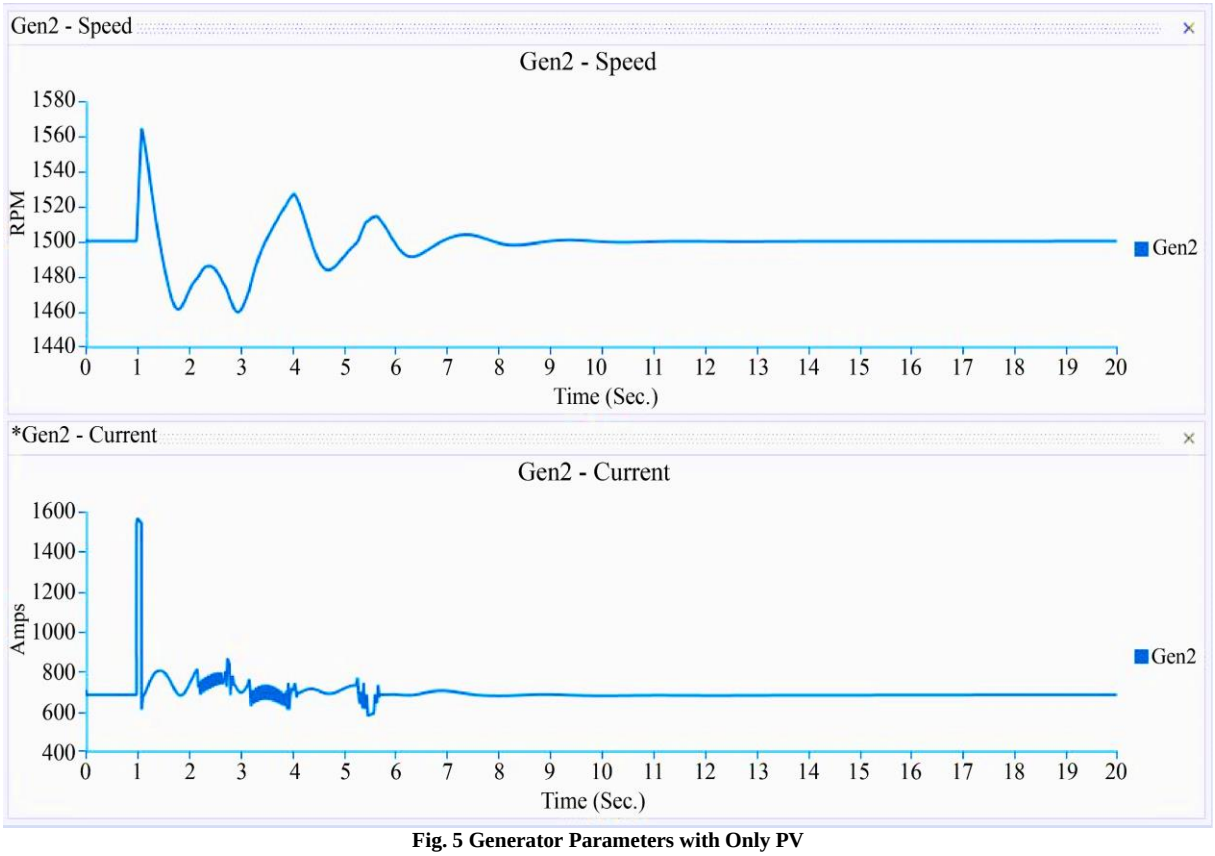

Fig. 5 Generator Parameters with Only PV

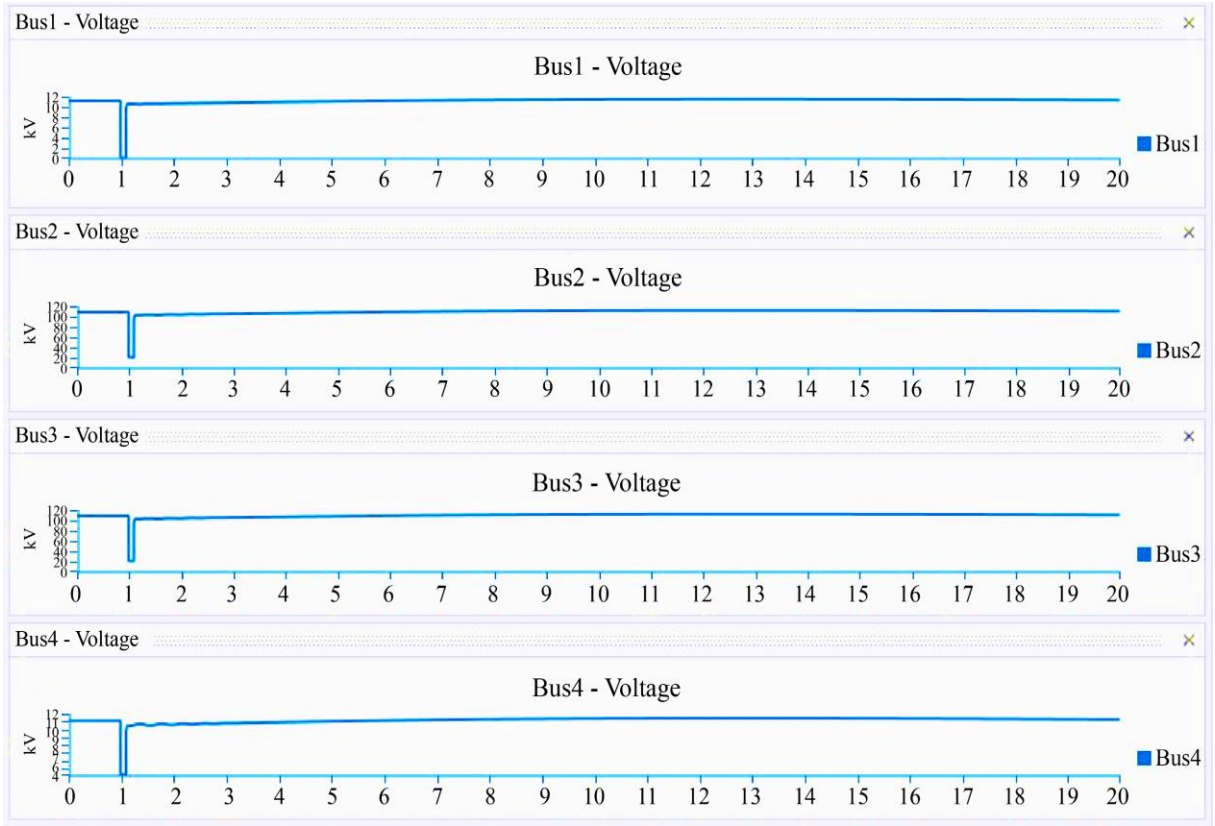

Fig. 6 Bus Voltages without PV FACTS

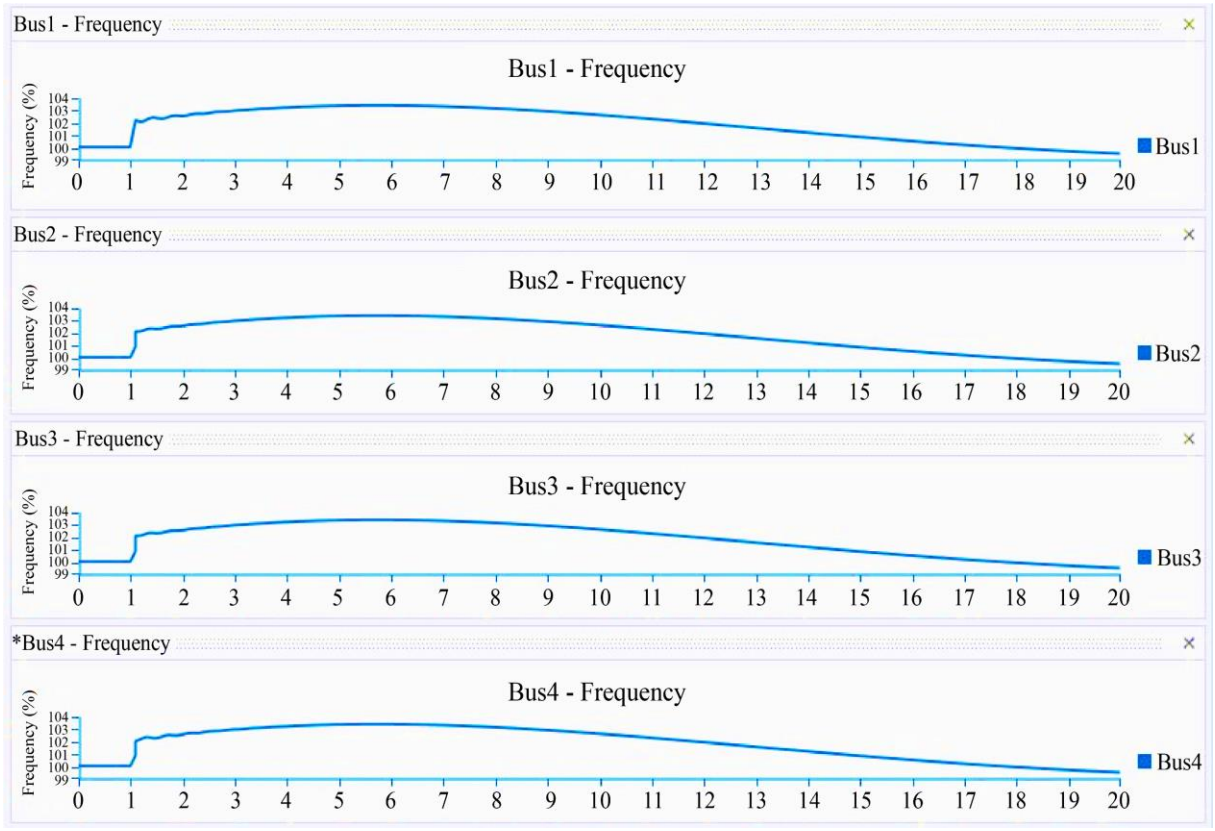

Fig. 7 Bus Frequency without PV FACTS

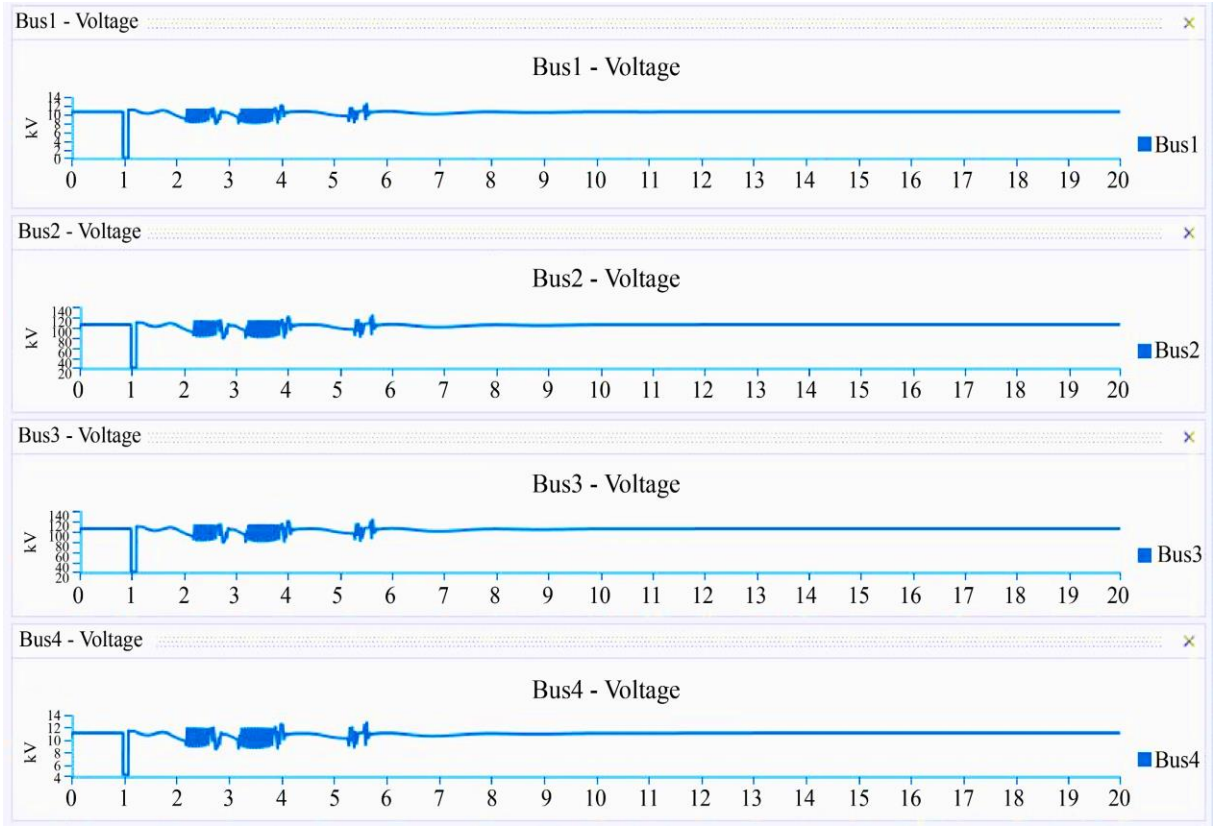

Fig. 8 Bus Voltages with only PV

Fig. 9 Bus Frequency with only PV

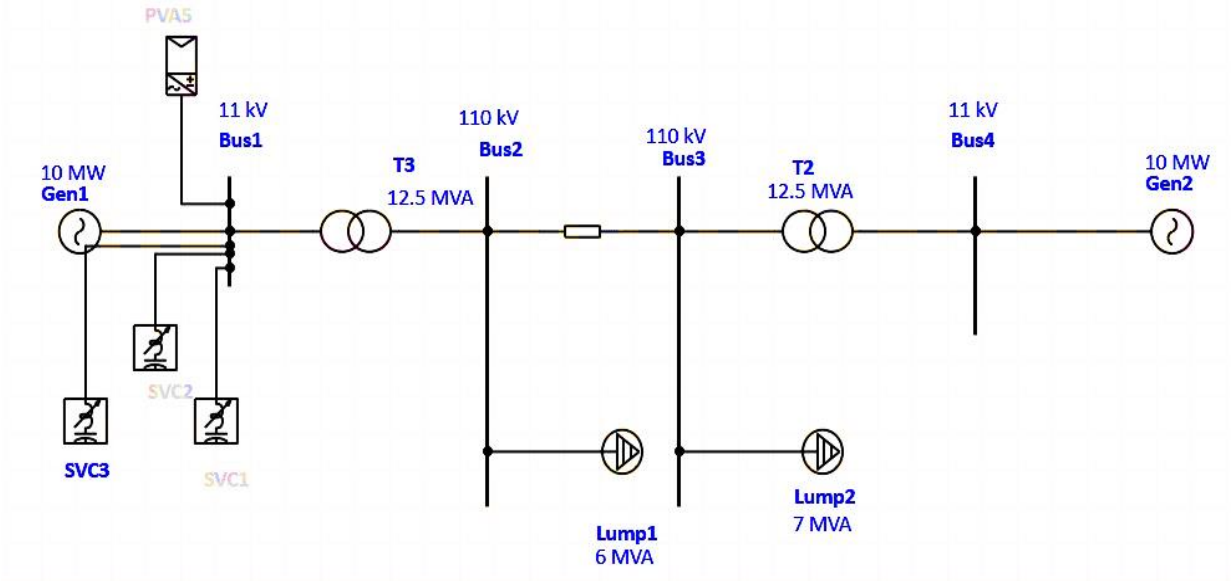

Fig. 10 Line Diagram of Test System in ETAP using Different SVC Types of Controller Model

Along with the generator speed and current, the proposed work also focused on the variation in the bus voltage magnitude and frequency concerning time. Earlier, excluding PV and FACTS, it has been seen that there is a dip in voltage for fault interval.

However, after that immediately, the voltage recovered to its slightly lower value than that of the before commencement of the fault, as can be seen in Figure 6. Whereas frequency disturbs initially, it is slightly increased for 3-4 seconds and then adopts the same pattern with a decrement in the frequency for the next few seconds.

Almost the same graph pattern reflected on each bus can be observed in Figure 7. After incorporating PV into the system, it is observed that the disturbance occurred in the system voltage and frequency, as shown in Figures 8 and 9, respectively. It is seen that the system voltage at each bus and frequency get disturbed because of this insertion of PV into the system.

To overcome the effect observed due to the addition of PV to the test system. We have introduced one of the popular FACTS devices in line with the PV System, i.e. SVC nearby generating unit can be seen in Figure 10.

6.1. SVC Control Model - Type1

Initially, in the above model, the SVC Type 1 controller is Enabled. Where control scheme shown in Figure 11 has been implemented.

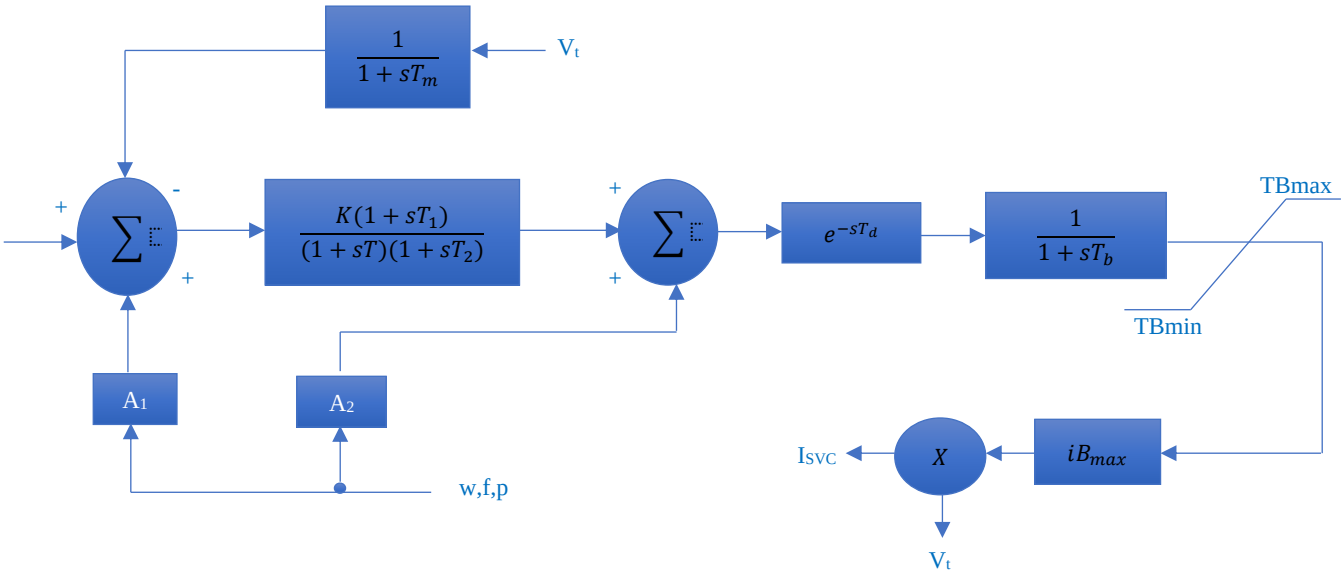

Fig. 11 SVC Control Model - Type1

Where Tm, Tb, and Td stand for the measurement, time, and delay constant of a thyristor phase control. The highest and lowest limits of susceptibility are indicated by T_{Bmax} and T_{Bmin}, respectively. The voltage regulator's gain, several time constants, and T1, T2, T, and K are represented correspondingly. However, A1 and A2 indicate additional signal enhancements that are used for control. After connecting the SVC Type 1 controller along with PV into the test system, all the graphs of Generator speed, bus voltage, frequency, and current have been observed concerning the time shown in Figures 12, 13, and 14 respectively.

For generator speed and current, it is observed that the system peak change in magnitude is almost the same but the time to recover the system becomes faster than in the previous case without the FACTS device. Similarly, bus voltage at each bus also recovers quicker due to the insertion of SVC as s FACTS into the system.

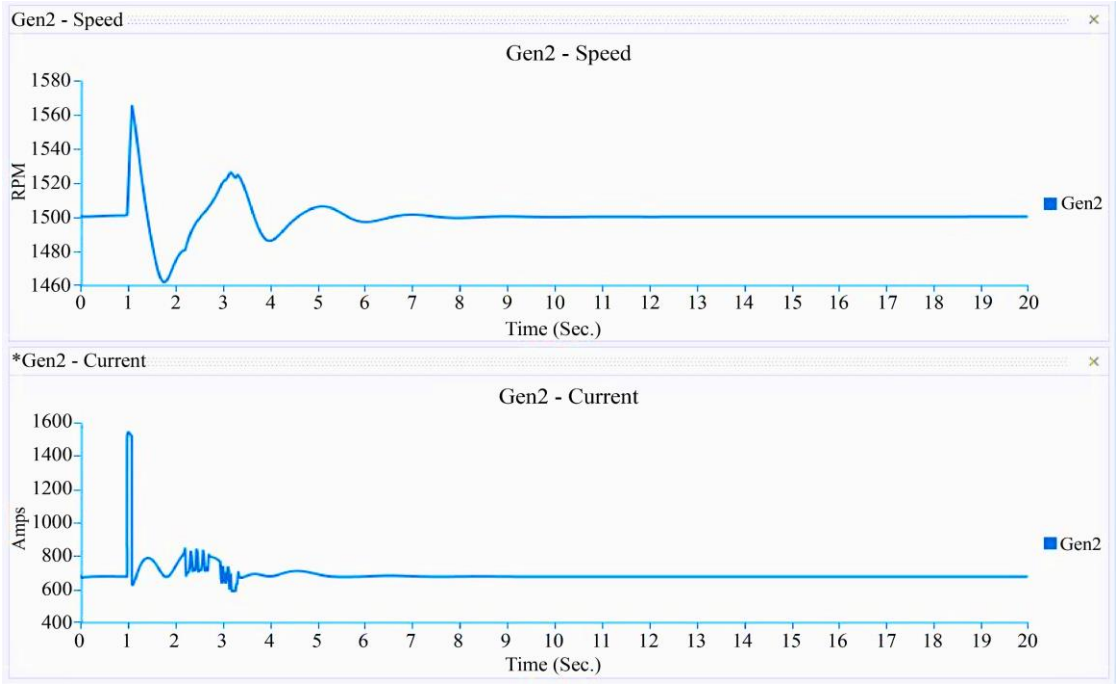

Fig. 12 Generator Parameters with PV FACTS

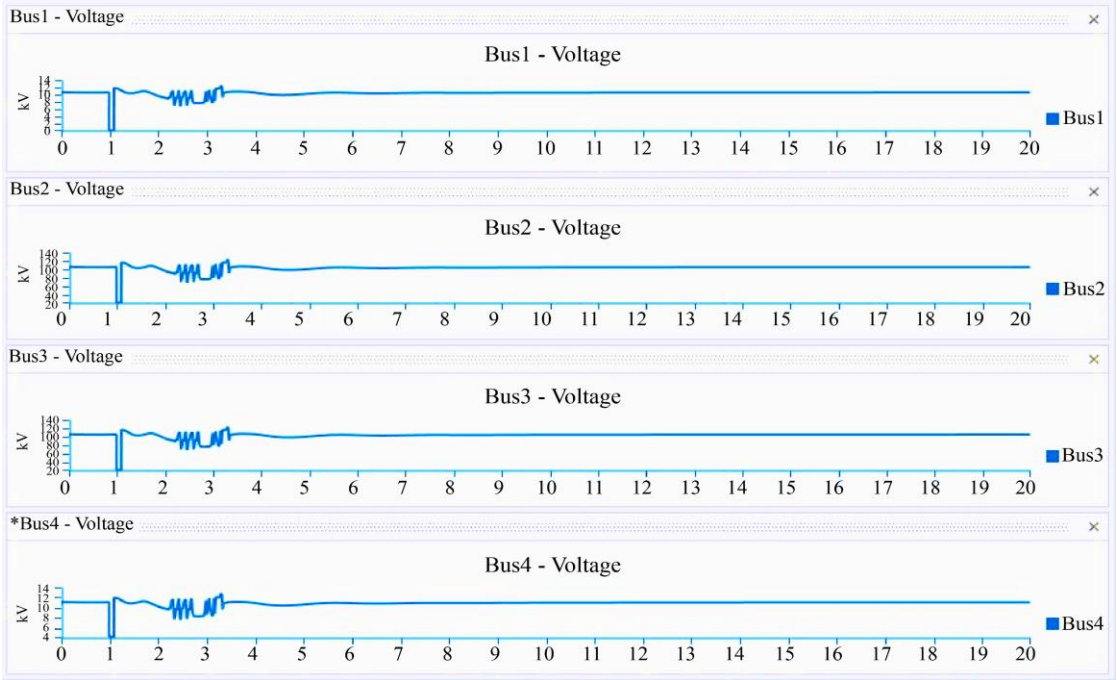

Fig. 13 Bus Voltages with PV FACTS

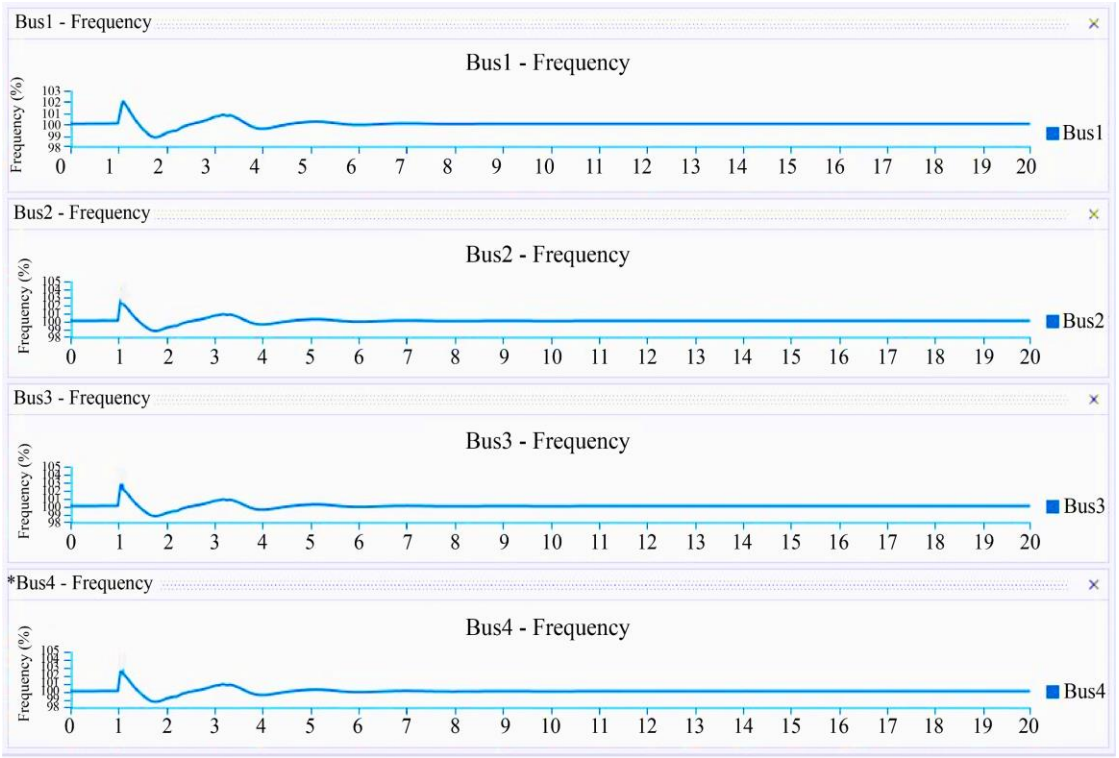

Fig. 14 Bus Frequency with PV FACTS

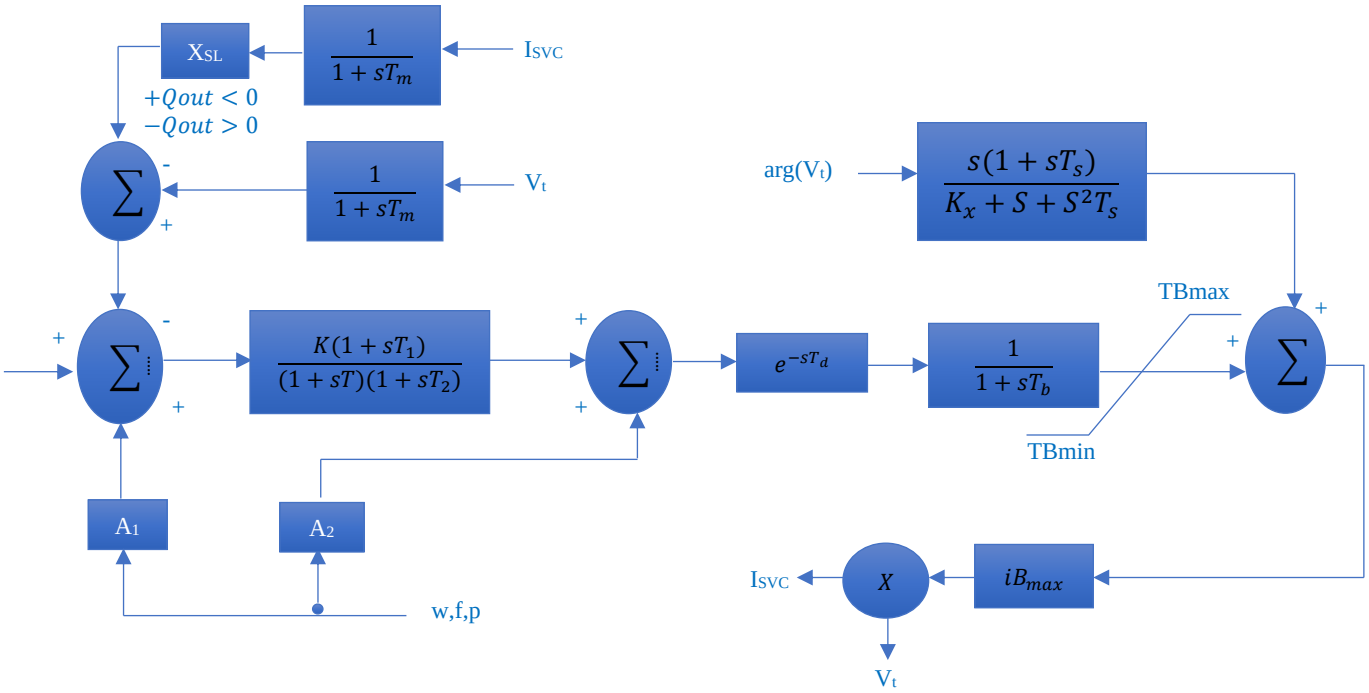

Fig. 15 SVC Control Model – Type2

6.2. SVC Control Model – Type2

The test model has been incorporated and enabled with the SVC Control Model - Type2, as illustrated in Figure 15 in the second stage. Once the SVC Type 2 Model controller and PV have been connected to the test system. Figures 16, 17, and 18 show, respectively, all the generator speed, bus voltage, frequency, and current graphs that have been observed with regard to time. Except for frequency, everything is within the acceptable range. In case of frequency, it exceeds the lower limit can be seen in Figure 18.

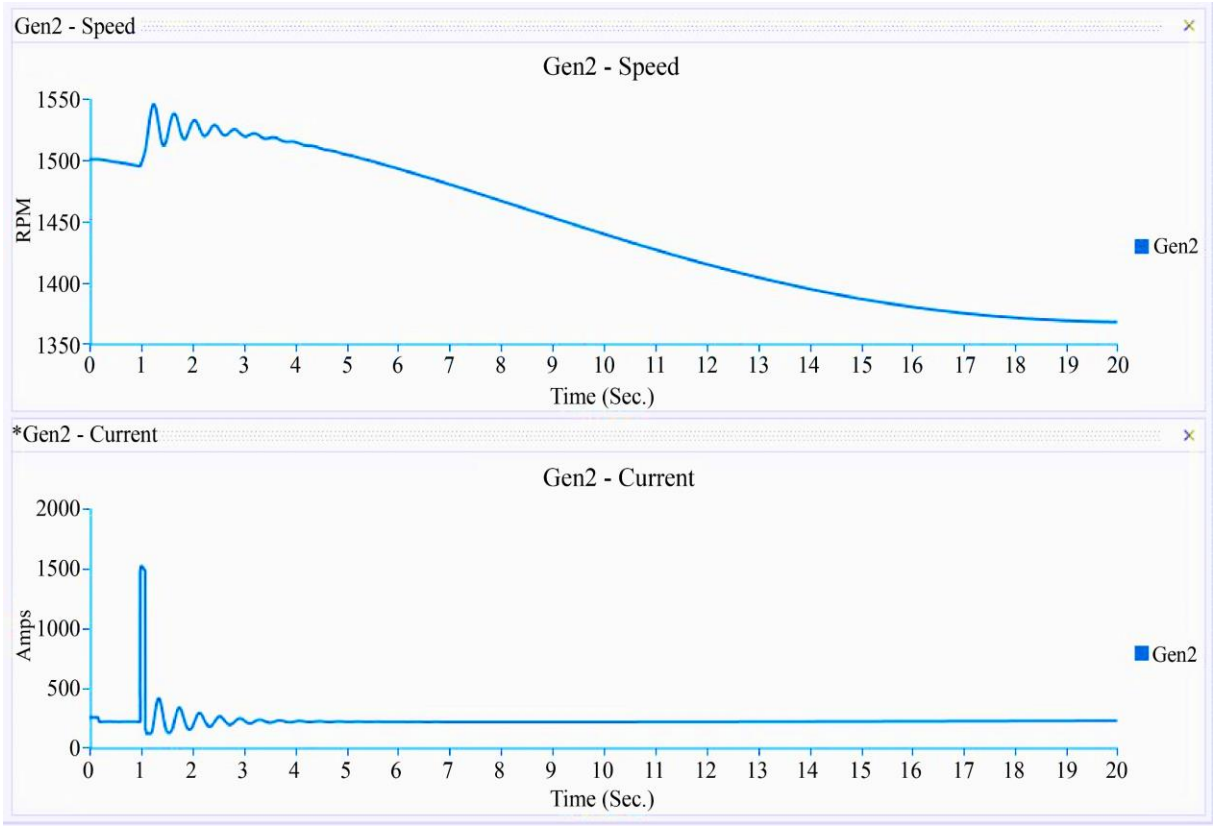

Fig. 16 Generator Parameters with PV FACTS

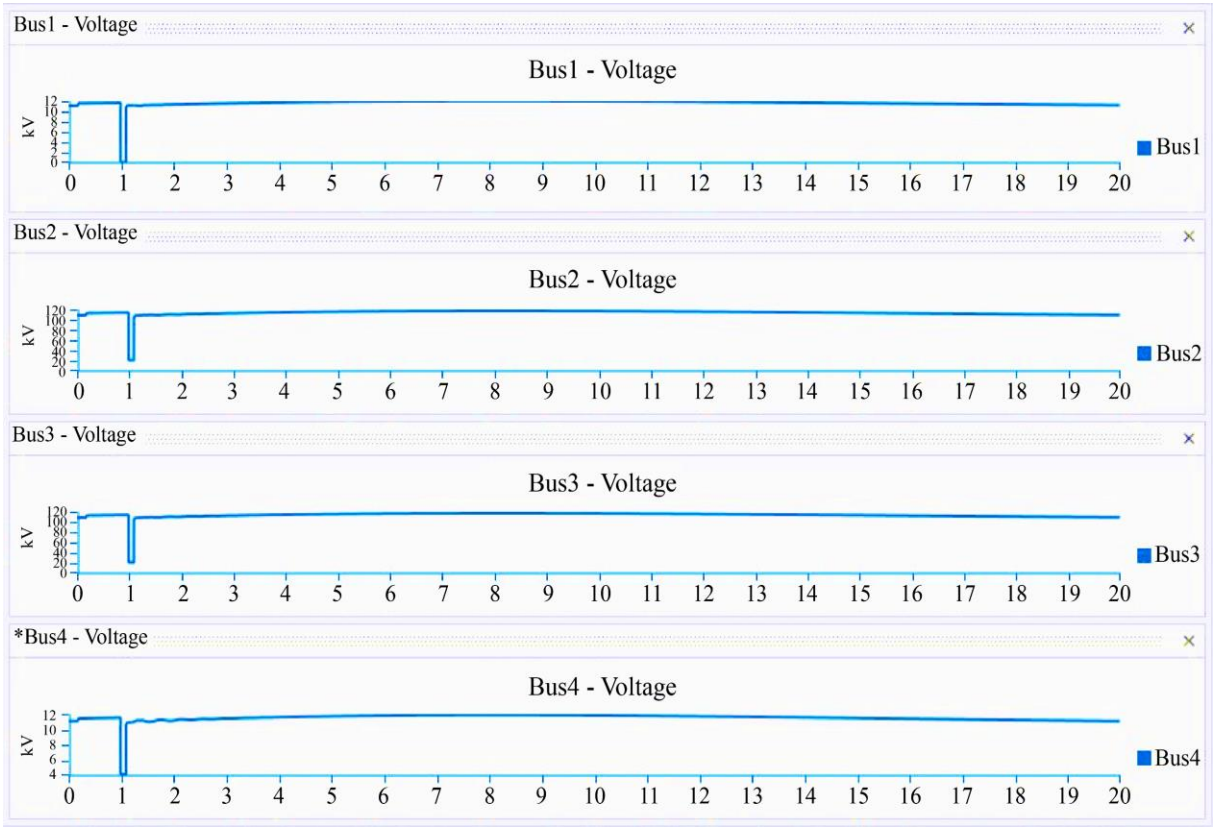

Fig. 17 Bus Voltages with PV FACTS

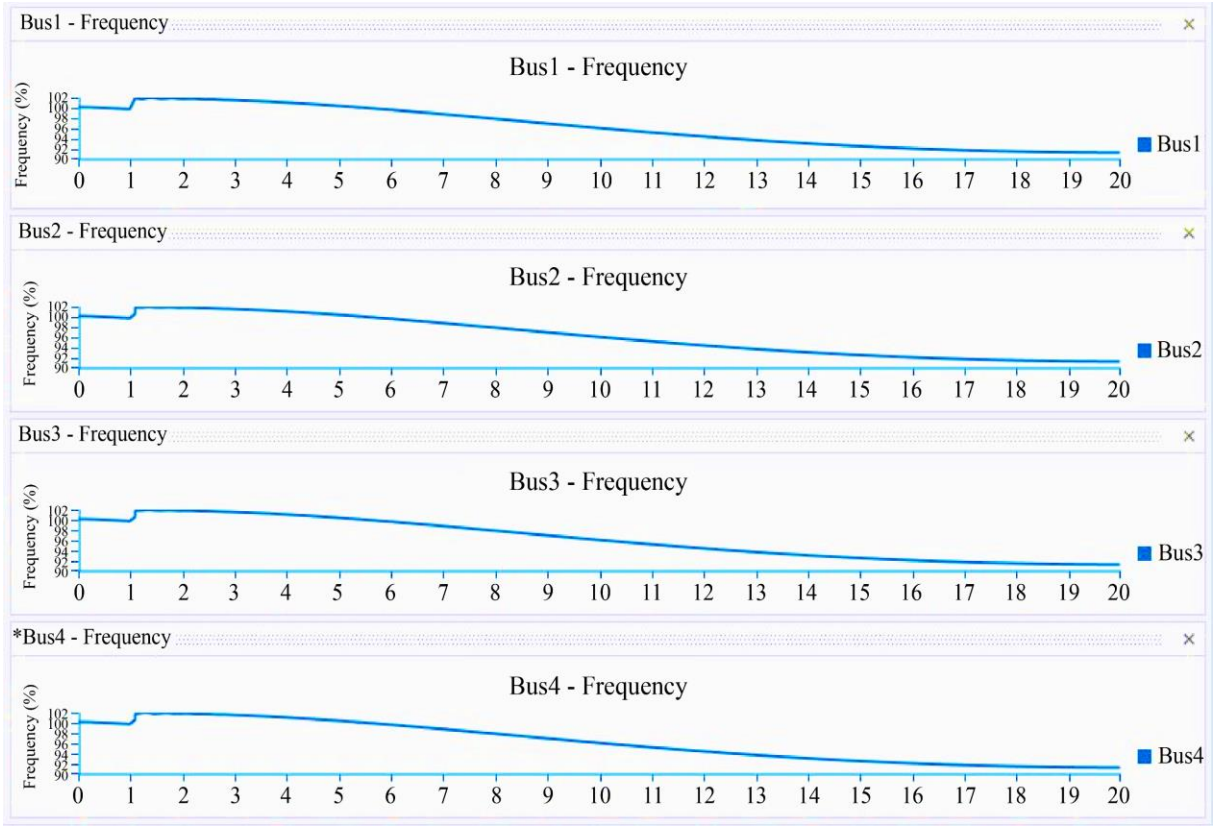

Fig. 18 Bus Frequency with PV FACTS

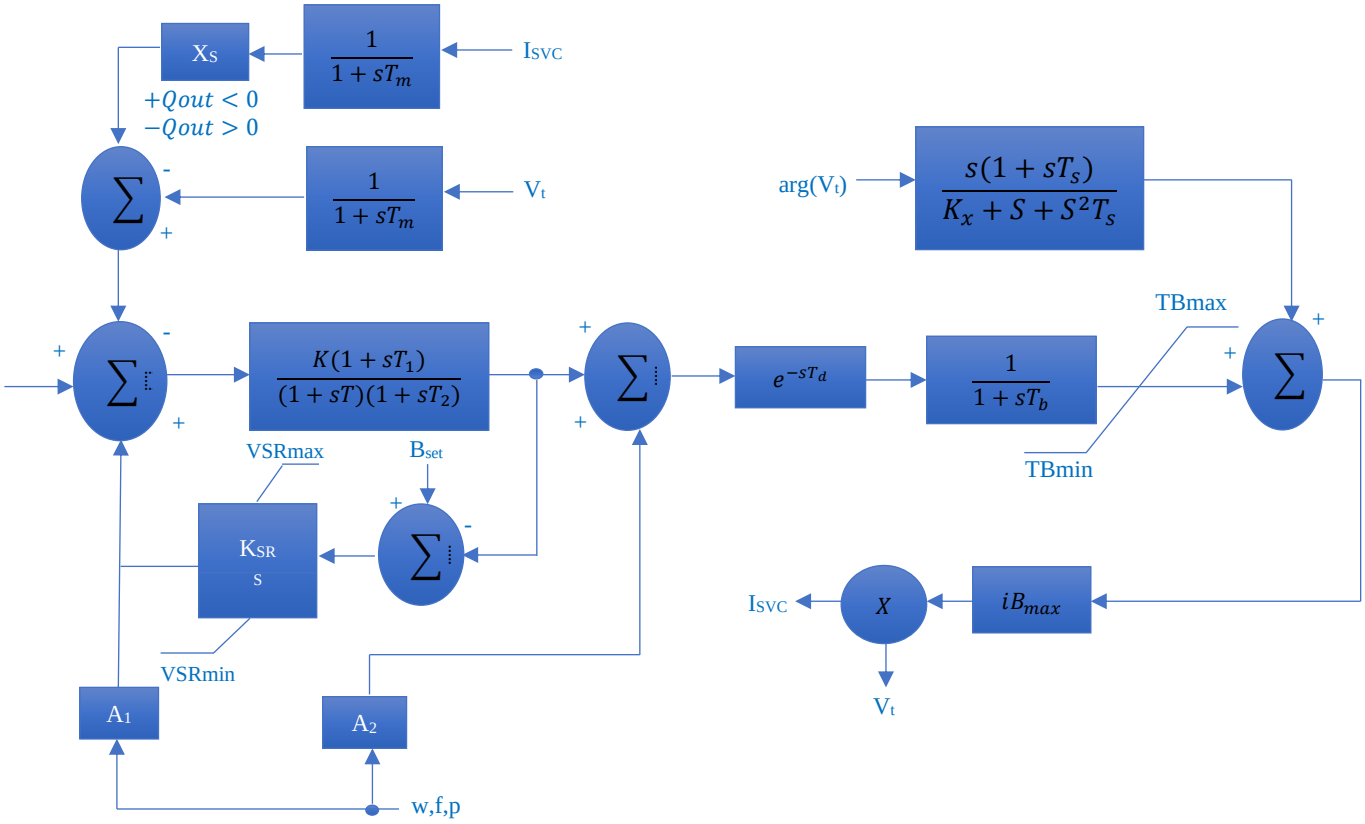

Fig. 19 SVC Control Model – Type3

6.3. SVC Control Model – Type3

Finally, the test model incorporates and enables the SVC Control Model – Type3, as depicted in Figure 19.

The test system's SVC Type 3 Model controller and PV have been connected. According to the time graphs depicted in Figures 20, 21, and 22, all generator speed, bus voltage, frequency, and current data have been obtained.

Almost the same nature of results was found and a similar decline is there for frequency after incorporating Type 3 controller.

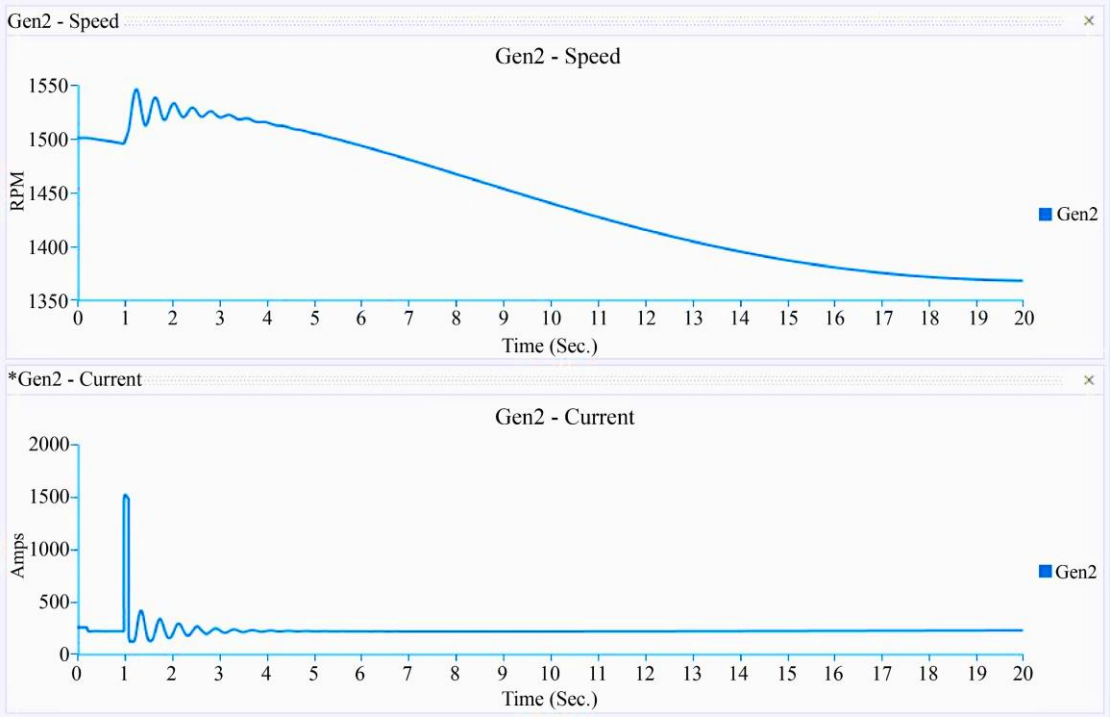

Fig. 20 Generator Parameters with PV FACTS

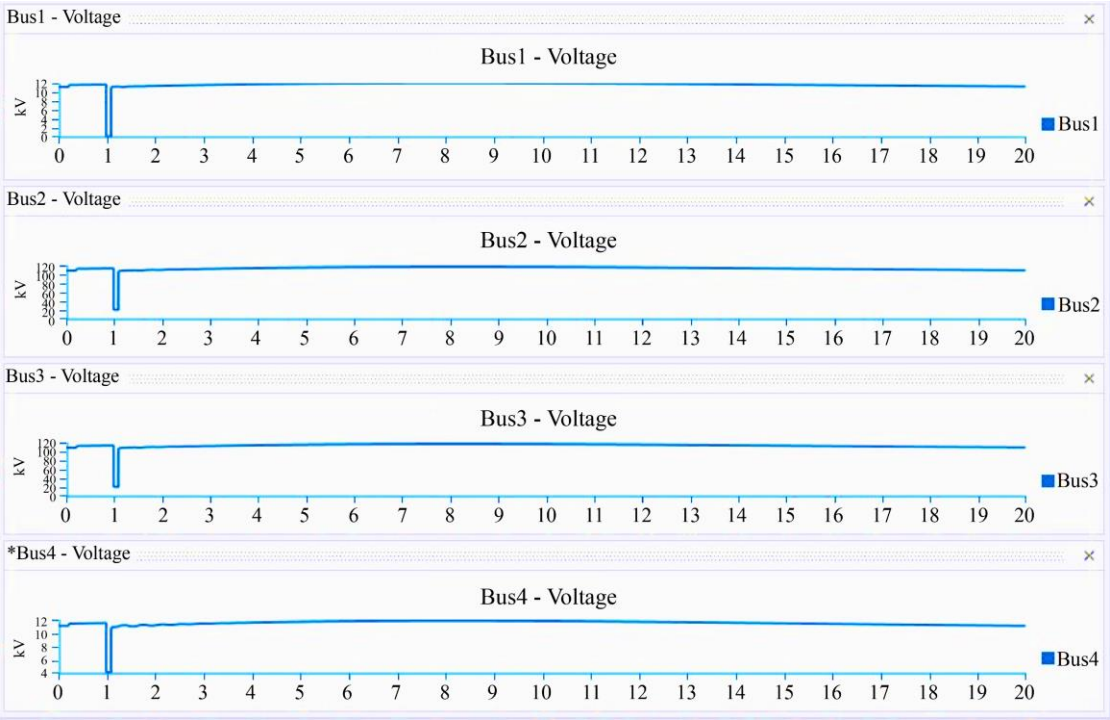

Fig. 21 Bus Voltages with PV FACTS

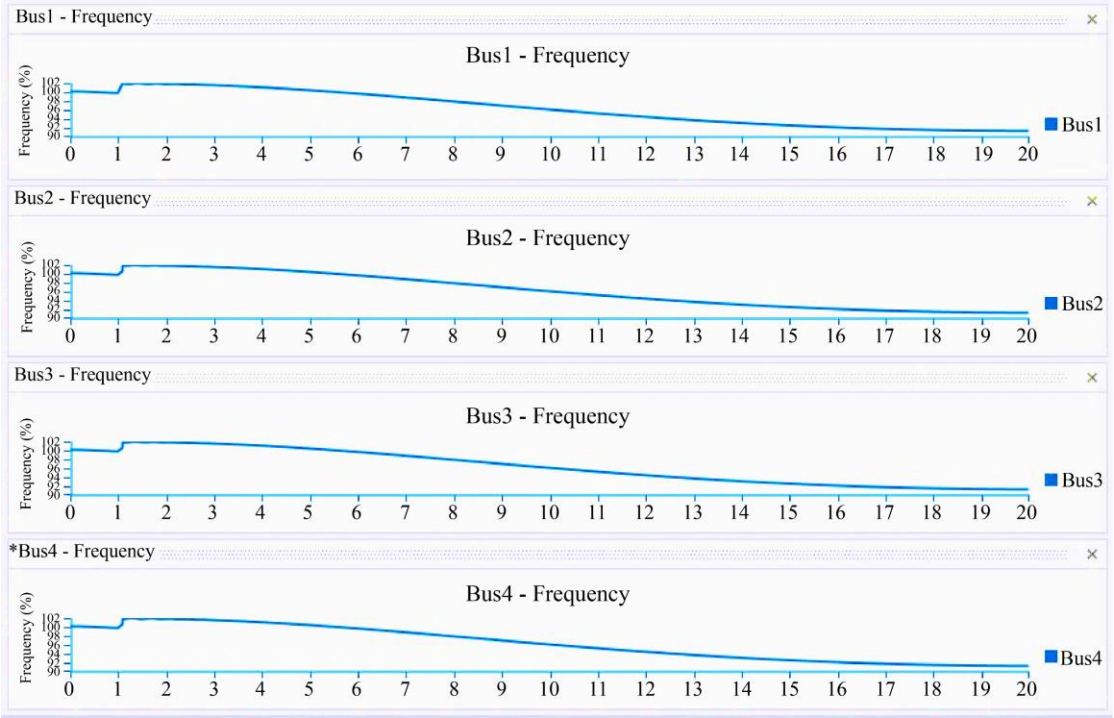

Fig. 22 Bus Frequency with PV FACTS

Table 2. Comparison of system parameters with and without FACTS Device

System Parameter	Parameter peak magnitude without SVC	Time required to restore the system	Parameter peak magnitude with SVC Type 1	Time required to restore the system
Speed	1565 rpm	8 Sec	1565 rpm	6 Sec
Current	1595 A	6 Sec	1595 A	4 Sec
Voltage	100	5 Sec	100	3 Sec
Frequency	106 %	7 Sec	103 %	4 Sec

Comparing all of the responses from each Type 1, 2, and 3, it can be seen that the Type 1 controller offers the greatest outcomes and achieves stability rapidly in terms of voltage, rotor angle, and, most significantly, frequency. All the results of these before and after application SVC type 1 along with PV are summarized in Table 2, which compares the test system on the basis of voltage and generator speed with and without the FACTS (SVC) device.

Finally, the change in percentage frequency with the addition of FACTS needs to be highlighted as the most significant aspect of these data. One can see from Table 2 and the frequency versus time graph that the addition of FACTS reduces the percentage frequency change from 106 to 103. It indicates a favorable effect that results in speedy operation.

7. Conclusion

ETAP was initially utilized to replicate the test system without PV and FACTS. After that, the speed and voltage waveforms were erratic with PV in the system. Wherever PV is added to the system, speed and voltage slightly vary but frequency surpasses its limit of 105%, and this is where the biggest influence was seen. The system is susceptible to instability, but this atypical unstable state may be addressed when SVC is used as a FACTS controller close to the generating unit. Considering the Type 1, 2, and 3 control models system regains its normal values. Among all the controller models, Type 1 model results are quite more promising than others, specifically in terms of frequency the waveform and table of the simulation results state and show that frequency is kept under control, or around 102%. However, other variables continue to operate steadily and more quickly than in prior instances. Ultimately, using SVC as a FACTS device, total system stability was enhanced.

Acknowledgments

The author would like to thank Professor Dr. L. D. Arya for giving valuable suggestions and guidance throughout the manuscript's preparation period. I also want to thank co-author Dr. Santosh S. Raghuwanshi and Medi-caps University, Indore (M.P), India, for providing a research facility at the campus.

References

[1] Prabha Kundur, *Power System Stability and Control*, McGraw-Hill Education, pp. 1-1176 1994. [Publisher Link]

[2] Prabha Kundur et al., "Definition and Classification of Power System Stability IEEE/CIGRE Joint Task Force on Stability Terms and Definitions," *IEEE Transactions on Power Systems*, vol. 19, no. 3, pp. 1387-1401, 2004. [CrossRef] [Google Scholar] [Publisher Link]

[3] Syed Bilal Qaiser Naqvi, Shailendra Kumar, and Bhim Singh, "Weak Grid Integration of a Single-Stage Solar Energy Conversion System with Power Quality Improvement Features Under Varied Operating Conditions," *IEEE Transactions on Industry Applications*, vol. 57, no. 2, pp. 1303-1313, 2021. [CrossRef] [Google Scholar] [Publisher Link]

[4] Shuaihu Li et al., "DNN-Based Distributed Voltage Stability Online Monitoring Method for Large-Scale Power Grids," *Frontiers in Energy Research*, vol. 9, pp. 80-88, 2021. [CrossRef] [Google Scholar] [Publisher Link]

[5] Rafat Aljarrah et al., "Research on the Impact of 100% PV Penetration in Power Distribution Systems," *2022 International Engineering Conference on Electrical, Energy, and Artificial Intelligence (EICEEAI)*, Zarqa, Jordan, pp. 1-5, 2022. [CrossRef] [Google Scholar] [Publisher Link]

[6] Aiman Abd Elkader Tawfiq et al., "Optimal Reliability Study of Grid-Connected PV Systems Using Evolutionary Computing Techniques," *IEEE Access*, vol. 9, pp. 42125-42139, 2021. [CrossRef] [Google Scholar] [Publisher Link]

[7] Ram Shankar Yallamilli, Thrinadh Dwibhashyam, and Kondalarao Bavisetti, "Weak Grid Integrated PV Plant Design Considerations for Improved Voltage Stability," *2022 22nd National Power Systems Conference (NPSC)*, New Delhi, India, pp. 59-64, 2022. [CrossRef] [Google Scholar] [Publisher Link]

[8] Amirhossein Sajadi et al., "Dynamics and Stability of Power Systems with High Shares of Grid-Following Inverter-Based Resources: A Tutorial," *IEEE Access*, vol. 11, pp. 29591-29613, 2023. [CrossRef] [Google Scholar] [Publisher Link]

[9] Xilin Li et al., "Nonlinear Modeling and Stability Analysis of Grid-Tied Paralleled-Converters Systems Based on the Proposed Dual-Iterative Equal Area Criterion," *IEEE Transactions on Power Electronics*, vol. 38, no. 6, pp. 7746-7759, 2023. [CrossRef] [Google Scholar] [Publisher Link]

[10] Guangyu Wang et al., "Transient Synchronization Stability of Grid-Forming Converter During Grid Fault Considering Transient Switched Operation Mode," *IEEE Transactions on Sustainable Energy*, vol. 14, no. 3, pp. 1504-1515, 2023. [CrossRef] [Google Scholar] [Publisher Link]

[11] Tong Wang et al., "Adaptive Damping Control Scheme for Wind Grid-Connected Power Systems With Virtual Inertia Control," *IEEE Transactions on Power Systems*, vol. 37, no. 5, pp. 3902-3912, 2022. [CrossRef] [Google Scholar] [Publisher Link]

[12] Himanshu Jain et al., "Grid-Supportive Loads-A New Approach to Increasing Renewable Energy in Power Systems," *IEEE Transactions on Smart Grid*, vol. 13, no. 4, pp. 2959-2972, 2022. [CrossRef] [Google Scholar] [Publisher Link]

[13] Yahong Chen et al., "Small-Signal System Frequency Stability Analysis of the Power Grid Integrated with Type-II Doubly-Fed Variable Speed Pumped Storage," *IEEE Transactions on Energy Conversion*, vol. 38, no. 1, pp. 611-623, 2023. [CrossRef] [Google Scholar] [Publisher Link]

[14] Anuprabha Nair et al., "An Investigation of Grid Stability and a New Design of Adaptive Phase-Locked Loop for Wind-Integrated Weak Power Grid," *IEEE Transactions on Industry Applications*, vol. 58, no. 5, pp. 5871-5884, 2022. [CrossRef] [Google Scholar] [Publisher Link]

[15] Zikang Li et al., "Fast Power System Event Identification Using Enhanced LSTM Network with Renewable Energy Integration," *IEEE Transactions on Power Systems*, vol. 36, no. 5, pp. 4492-4502, 2021. [CrossRef] [Google Scholar] [Publisher Link]

[16] Anindya Bharatee, Pravat K. Ray, and Arnab Ghosh, "A Power Management Scheme for Grid-Connected PV Integrated with Hybrid Energy Storage System," *Journal of Modern Power Systems and Clean Energy*, vol. 10, no. 4, pp. 954-963, 2022. [CrossRef] [Google Scholar] [Publisher Link]

[17] Jing Ma et al., "Renewable Energy Integrated HVDC Power System Modeling for Transient Frequency Stability Online Assessment," *2022 7th International Conference on Power and Renewable Energy (ICPRE)*, Shanghai, China, pp. 1-5, 2022. [CrossRef] [Google Scholar] [Publisher Link]

[18] Kabulo Loji, Nomhle Loji, and Musasa Kabeya, "Flexibility Assessment of a Solar PV Penetrated IEEE 9-Bus System Using Dynamic Transient Stability Evaluation," *2022 IEEE PES/IAS PowerAfrica*, Kigali, Rwanda, pp. 1-5, 2022. [CrossRef] [Google Scholar] [Publisher Link]

[19] Yuhan Guo et al., "Small-Signal Stability Modeling and Analysis of Power System with Integrated Photovoltaic Energy Storage," *2022 IEEE 6th Conference on Energy Internet and Energy System Integration (EI2)*, Chengdu, China, pp. 2850-2856, 2022. [CrossRef] [Google Scholar] [Publisher Link]

[20] Dhirajsing Rughoo et al., "Analysis of the Power System Stability upon Integration of PV System into the National Grid of the Island of Mauritius," *2022 International Conference on Electrical, Computer, Communications and Mechatronics Engineering (ICECCME)*, Maldives, Maldives, pp. 1-5, 2022. [CrossRef] [Google Scholar] [Publisher Link]

[21] Qianjin Zhang et al., "Stability Problems of PV Inverter in Weak Grid: A Review," *IET Power Electronics*, vol. 13, no.11, pp. 2165-2174, 2020. [CrossRef] [Google Scholar] [Publisher Link]

[22] Muhammad A. Tayyab, and Eduard Muljadi, "Dynamic Stability of Large-Scale Photovoltaic Based Generation Integration into Power Systems," *2022 5th International Conference on Power Engineering and Renewable Energy (ICPERE)*, Bandung, Indonesia, pp. 1-6, 2022. [CrossRef] [Google Scholar] [Publisher Link]

[23] Jafar Sarbazi et al., "Effects of Photovoltaic Power Plants Grid Code Requirements on Transient Stability," *2022 12th Smart Grid Conference (SGC)*, Kerman, Iran, pp. 1-7, 2022. [CrossRef] [Google Scholar] [Publisher Link]

[24] U. Shriya, and H.S. Veena, "Increasing Grid Power Transmission Using PV-STATCOM," *2021 6th International Conference for Convergence in Technology (I2CT)*, Maharashtra, India, pp. 1-5, 2022. [CrossRef] [Google Scholar] [Publisher Link]

[25] Godfrey Gladson Moshi, Erick Vincent Mgaya, and Sithole Edwin Mwakatage, "Grid Connection Studies for PV Power Plant in Medium Voltage Distribution Network," *2023 23rd International Scientific Conference on Electric Power Engineering (EPE)*, Brno, Czech Republic, pp. 1-6, 2022. [CrossRef] [Google Scholar] [Publisher Link]

[26] Arjun Tyagi et al., "Optimal Utilization of Reactive Power Capabilities of Distributed Solar PV Inverter," *2022 22nd National Power Systems Conference (NPSC)*, New Delhi, India, pp. 30-34, 2022. [CrossRef] [Google Scholar] [Publisher Link]

[27] Bukola Babatunde Adetokun, Joseph Olorunfemi Ojo, and Christopher Maina Muriithi, "Reactive Power-Voltage-Based Voltage Instability Sensitivity Indices for Power Grid with Increasing Renewable Energy Penetration," *IEEE Access*, vol. 8, pp. 85401-85410, 2020. [CrossRef] [Google Scholar] [Publisher Link]

[28] K.K. Mahapatra, A. Ghosh, and S.R. Doradla, "Simplified Model for Control Design of STATCOM Using Three-Level Inverter," *Proceedings of IEEE TENCON '98. IEEE Region 10 International Conference on Global Connectivity in Energy, Computer, Communication and Control (Cat. No.98CH36229)*, New Delhi, India, pp. 536-539, 1998. [CrossRef] [Google Scholar] [Publisher Link]

[29] H. Abdel-Gawad, and Vijay K. Sood, "Overview of Connection Topologies for Grid-Connected PV systems," *2014 IEEE 27th Canadian Conference on Electrical and Computer Engineering (CCECE)*, Toronto, ON, Canada, pp. 1-8, 2014. [CrossRef] [Google Scholar] [Publisher Link]

[30] Muhammad H. Rashid, *Power Electronics Handbook*, Elsevier Science, pp. 1-1362, 2011. [Publisher Link]